38p

NASA CONTRACTOR REPORT

HIGH-EFFICIENCY NARROW-BAND LASER PUMP

PREPARED BY S. A. OCHS AND J. I. PANKOVE (Project Engineer)

APPROVED BY M. B. LEWIS

FINAL REPORT

FOR THE PERIOD

JANUARY 24, 1963 TO FEBRUARY 28, 1964

Prepared under Contract No. NAS 8-5219

RADIO CORPORATION OF AMERICA
RCA LABORATORIES
PRINCETON, NEW JERSEY

for

NATIONAL AERONAUTICS & SPACE ADMINISTRATION • HUNTSVILLE, ALA. • FEBRUARY 1964

NASA CONTRACTOR REPORT

HIGH-EFFICIENCY NARROW-BAND LASER PUMP

PREPARED BY S. A. OCHS AND J. I. PANKOVE (Project Engineer)

APPROVED BY H. R. LEWIS

FINAL REPORT

FOR THE PERIOD
JANUARY 24, 1963 TO FEBRUARY 28, 1964

Prepared under Contract No. NAS 8-5219

RADIO CORPORATION OF AMERICA
RCA LABORATORIES
PRINCETON, NEW JERSEY

for

NATIONAL AERONAUTICS & SPACE ADMINISTRATION • HUNTSVILLE, ALA. • FEBRUARY 1964

TABLE OF CONTENTS

LIST OF ILLUSTRATIONS

LIST OF ILLUSTRATIONS (Continued)

PURPOSE

The objective of this program is to carry out research on the pumping of a continuously operating insulator laser by a semiconductor light source.

ABSTRACT

It was decided to study the pumping of a $CaF_2:Dy^{2+}$ laser by means of injection luminescence from $GaAs_{.73}P_{.27}$ pn junctions. Diodes were made from such an alloy grown epitaxially on (100) GaAs. External conversion efficiencies of about one photon leaving the diode per 100 electrons traversing the junction were obtained.

One hundred diodes were connected in series, in ten linear arrays, and were arranged around the laser rod. This assembly was immersed in liquid helium cooled below the lambda point. Single current pulses caused lasing when the total light output of the diodes was about 0.1 watt. An appreciable delay was found between the beginning of the current pulse and the onset of lasing. Heating effects limited the lasing action to about 0.2 second.

auth.

I. INTRODUCTION

Some of the most promising applications of lasers are in the fields of communications and radar. The spectral purity of the laser beam permits discriminating against background noise in a narrow-band receiver and the use of conventional heterodyning techniques. Also, the spatial coherence of the laser radiation makes it possible to form extremely narrow beams with a divergence sometimes measured in seconds of arc.

Laser action has been achieved by various means in solids, liquids, and gases. The characteristics of these devices vary widely and the selection of a particular device depends upon the requirements of the application. In many applications, it is important that the device be small and efficient. Laser systems which have appeared very promising in this respect are the solid-state lasers based on rare-earth ions in a crystalline host. These lasers, which are optically pumped, have been developed to the point where relatively little light is needed to yield laser action. In the best units the lasing threshold is reached when about a joule of radiant energy has been absorbed.

The light sources generally used for pumping (chiefly xenon, mercury, or tungsten lamps) produce radiation in a wide band of frequencies, i.e., essentially "white" light, of which only a small fraction is absorbed by the laser. This project was concerned with the development of a laser pump with a light output in a narrow band which is strongly absorbed by the laser crystal, so as to pump electrons into the laser level. Forward-biased semiconductor junctions produce such narrow-band radiation by the recombination of electrons and holes injected into the n and p regions, respectively. Recent developments in this field have yielded high conversion efficiencies from electrical to optical energy and have demonstrated the possibility of producing light of the desired wavelength through proper adjustment of the band gap of the semiconductor used. Since the input to these luminescent diodes is electrical, they require relatively small, simple power sources; and their output is modulated readily.

Lasing has been achieved in semiconductor diodes pumped by injection. However, such injection lasers are not likely to achieve the spectral purity of the insulator lasers considered above, because of the relatively small size of the injection lasers and their tendency to shift from mode to mode while lasing.

II. $CaF_2:Dy^{2+}$ LASER

Among optically pumped lasers, the lowest threshold has been obtained with divalent dysprosium in calcium fluoride.[1] Figure 1 indicates the energy level scheme of the $CaF_2:Dy^{2+}$. The individual levels within 8000 cm^{-1} of the

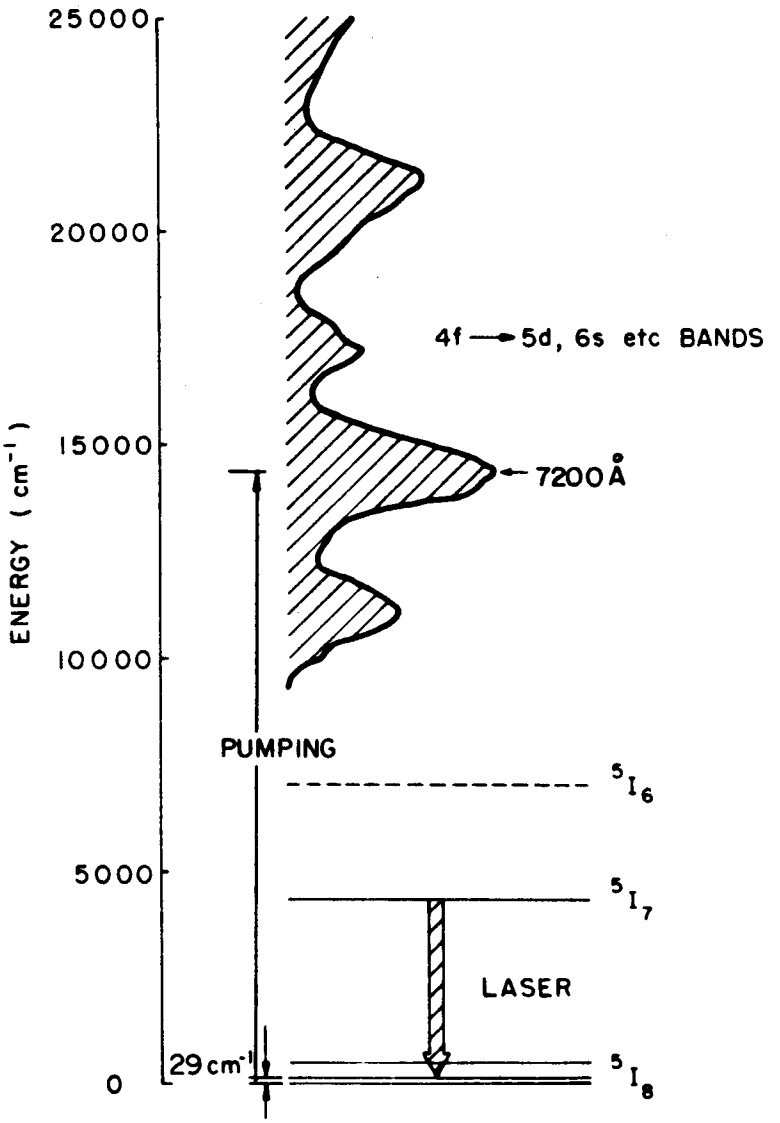

Fig. 1. Energy levels of $CaF_2:Dy^{2+}$.

ground state are 4f levels. The fluorescence spectrum of $CaF_2:Dy^{2+}$, shown in Figure 2, is due to transitions between these levels (from the $^5I_7$ to the

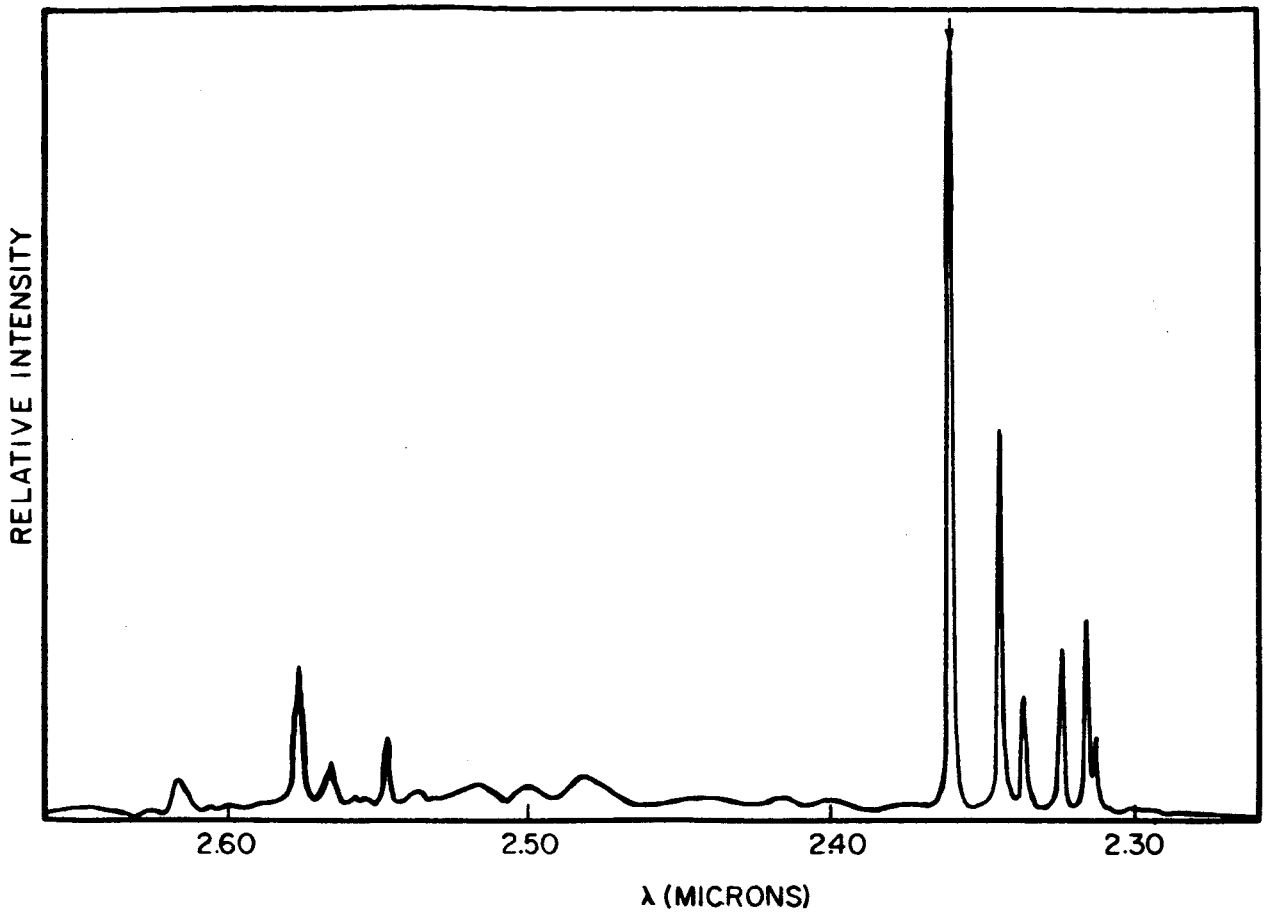

Fig. 2. Fluorescence spectrum of $CaF_2:Dy^{2+}$ at 77°K.

$^5I_8$ state). Since 4f-4f transitions are forbidden, according to quantum-mechanical selection rules, the levels in the ^5I multiplet are metastable and the fluorescence lines are very sharp. The $^5I_8$ level is split by the crystal field, causing several lines to appear in the fluorescence spectrum. The strongest line occurs at 2.36 μ (4236 cm^{-1}) and is due to a transition from the $^5I_7$ state to a level located 29 cm^{-1} above the ground state. By pumping electrons into the $^5I_7$ state, a population inversion can then be achieved quite easily and the 2.36-μ line can be stimulated into laser oscillation. Figure 1 also shows the broad bands, starting at 9,500 cm^{-1}, which correspond to the 4f-5d transitions. Light of energy greater than 9.500 cm^{-1}(i.e., of wavelength less than 10,500 Å) is therefore readily absorbed by the crystal, causing electrons to be excited to the 5d levels. Many of these electrons will then, by a radiationless transition, drop to the metastable $^5I_7$ state which is the upper laser level.

The laser which has just been described, originally was pumped by light containing a wide range of wavelengths (produced by Xe flash lamps, hot tungsten filaments, or the sun). The broad bands in the upper portion of Figure 1 essentially represent the absorption spectrum of divalent dysprosium in CaF_2 and they are drawn so as to indicate the relative absorption coefficient as a function of energy. It is seen that the light is not absorbed uniformly at all wave numbers. The greatest absorption takes place in a band centered at 13,900 cm^{-1} which corresponds to a wavelength of 7,200 Å and a photon energy of 1.72 eV. At an absorption coefficient of half the maximum value, the band extends from 6800 Å (1.81 eV) to 7500 Å (1.63 eV).

This project therefore, was aimed at developing a light source which produces radiation in a narrow range at 7,200 Å. It was expected that forward-biased pn junctions in an alloy containing 73% GaAs and 27% GaP would satisfy the requirements of such a laser pump.

III. INJECTION-LUMINESCENT DIODES

A. BACKGROUND

When a pn junction in a semiconductor crystal is biased in the forward direction, the electrons on the n side and holes on the p side can penetrate further into the space-charge region than in an unbiased junction. Now, if the carrier concentration is large (degenerate material) and the voltage across the pn junction is sufficiently strong to nearly overcome the junction potential, a substantial overlap of electrons and holes can occur in the junction region. Electron-hole pairs will recombine and produce photons whose energy is approximately equal to the width of the forbidden gap (see Figure 3).

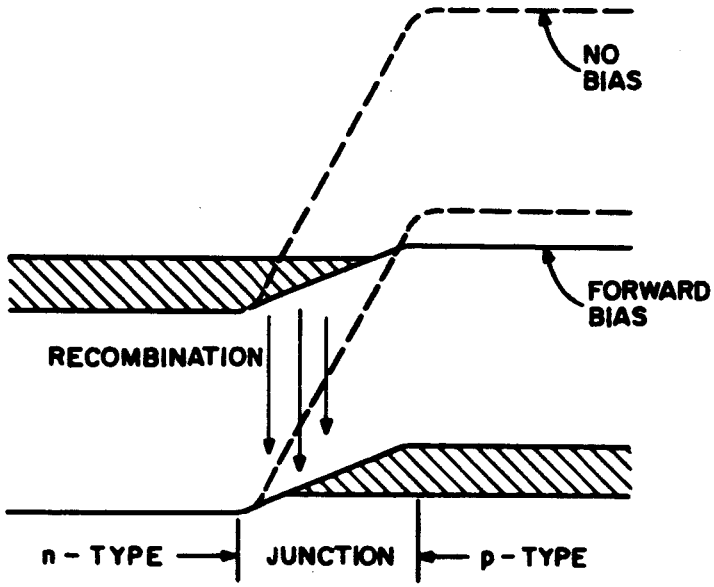

Fig. 3. Band diagram of forward-biased injection laser.

Such recombination radiation was found in degenerately doped gallium arsenide diodes[2] in which the injected carriers produce photons with essentially unity quantum efficiency. Due to the high index of refraction of GaAs (about 4.0 at the emitted wavelength) much of the radiation is totally reflected by the surface of the crystal. Rays inclined by more than 17° with respect to the normal to the surface are totally reflected; also, about one third of the radiation striking the surface with an angle smaller than 17° is reflected by the semiconductor-air interface. The radiation trapped in the crystal is converted into heat, and by raising the temperature of the crystal makes further radiative recombination somewhat less efficient. Because of the

above-mentioned total and partial reflections, only about 4 percent of the emitted photons leave the crystal through each flat surface. Curved surface and anti-reflection layers could be used to greatly improve the overall efficiency of the injection-electroluminescent device.

Radiative recombination has also been found in diodes made from GaAs-GaP alloy[3] with up to about 40-percent GaP content. Figure 4 shows the variation of the energy gap of a $GaAs_{1-x}P_x$ crystal as a function of the mole fraction x of GaP content. High quantum efficiencies are expected for values of x less than 0.5, corresponding to the region in which "direct" transitions occur, i.e., hole and electron have the same momentum before recombination.

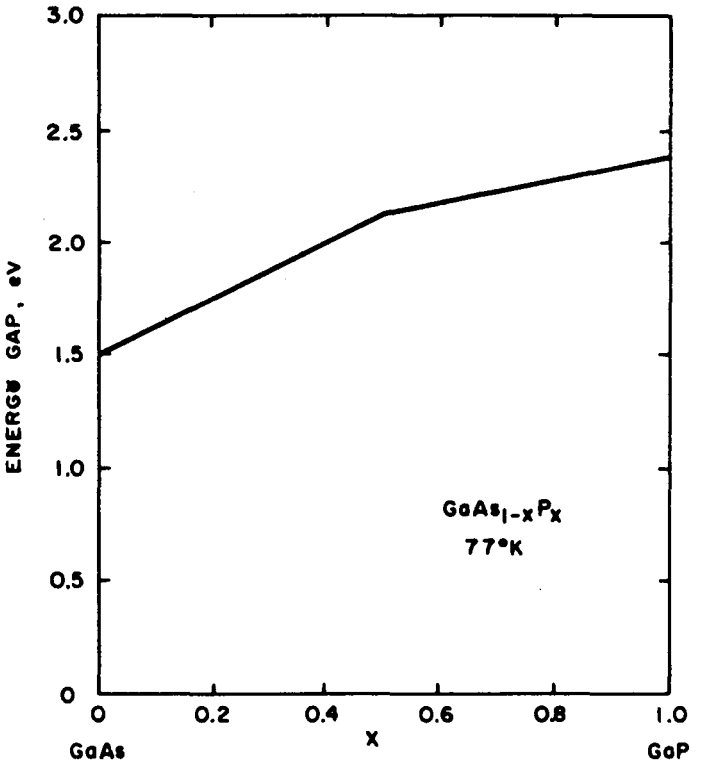

Fig. 4. Variation of energy gap with composition for $GaAs_{1-x}P_x$ at 77°K [after Ehrenreich, J. Appl. Phys. 32, 2155 (1961)].

B. DIODE FABRICATION

The diodes used in this project were made from tellurium-doped $GaAs_{1-x}P_x$ epitaxial layers grown on GaAs crystals. The alloy, together with the dopant, was transferred by vapor transport from a source wafer onto the GaAs substrate, which was about ten mils away from the source. This technique was perfected by G. E. Gottlieb and is described more fully in the Appendix.

Two kinds of source material were used. Most layers were grown from wafers cut from polycrystalline ingots made at RCA Laboratories. However, about twenty layers were grown from single-crystal $GaAs_{1-x}P_x$ wafers purchased from Merck & Co. There was no indication that any difference between various epitaxial layers was caused by the source material used. This may have been due to the fact that reproducibility in the diode behavior was rather poor, even for diodes made from layers grown under similar conditions and using the same source material. Early layers were grown on (111) crystal faces, but all of the later samples were grown on (100) faces since this made it easier to cleave the crystal into right-angled parallelepipeds. The carrier concentration was generally in the 10^{18} cm^{-3} range. The epitaxial deposit was typically 1/4 in. x 3/8 in. in area and from one to six mils thick. The total number of layers grown during this contract was about 240.

The epitaxial layer was lapped flat and polished in order that the zinc diffusion would result in a flat pn junction. After many variations of the diffusion conditions had been tried, it was found that relatively good and reliable results could be obtained when 0.3 mg of zinc, in the presence of 0.3 mg of arsenic, per cubic cm of ampule volume were diffused at 800°C for a half hour. Most diodes were made under approximately these conditions. The resultant p-type region has a fairly uniform depth of about one mil. A cross-sectional view of a $GaAs_{1-x}P_x$ layer which has been etched so as to delineate the pn junction is shown in Figure 5.

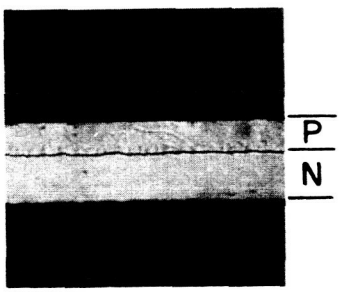

Fig. 5. Microphotograph of cleaved cross section of $GaAs_{1-x}P_x$ diode.

The diodes were then finished by the following process. The GaAs substrate was removed and the $GaAs_{1-x}P_x$ layer lapped down (from the n-type side) to a final thickness of about three mils. Tin was evaporated onto the n-type side and alloyed into the surface at about 600°C. Nickel and gold were then plated onto both sides. Finally, the wafers were cleaved into rectangular pieces, typically 10 mils x 20 mils in area, by rolling a metal bar over them parallel to the two [100] directions, or by pressing the edge of a razor blade against their surface.

Hall measurements on a typical sample of the n-type material (before zinc diffusion) showed it to have the following characteristics:

Carrier concentration = 2.2×10^{18} cm^{-3}
Resistivity = 5.4×10^{-13} ohm-cm
Mobility = 518 cm^2/volt-sec.

C. DIODE CHARACTERISTICS

Most of the tests were performed in liquid nitrogen, i.e., at approximately 77°K. Contacts were made either by pressure or with soldered joints. A typical current vs. voltage graph is shown in Figure 6. The saturation current

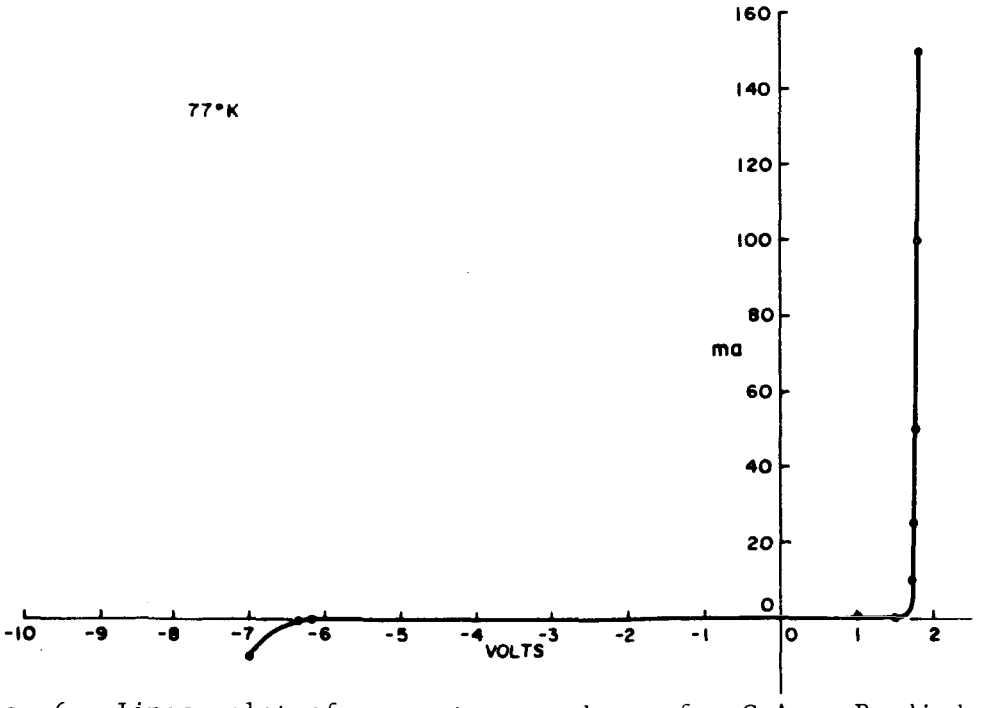

Fig. 6. Linear plot of current vs. voltage for $GaAs_{1-x}P_x$ diode.

is seen to be negligible. The diode can have a reverse bias (p-type negative) of several volts applied before breakdown current starts to flow. The forward current increases rapidly at the band-gap voltage. The current-voltage variation in this region is indicated more clearly in Figure 7. Here this logarithm of

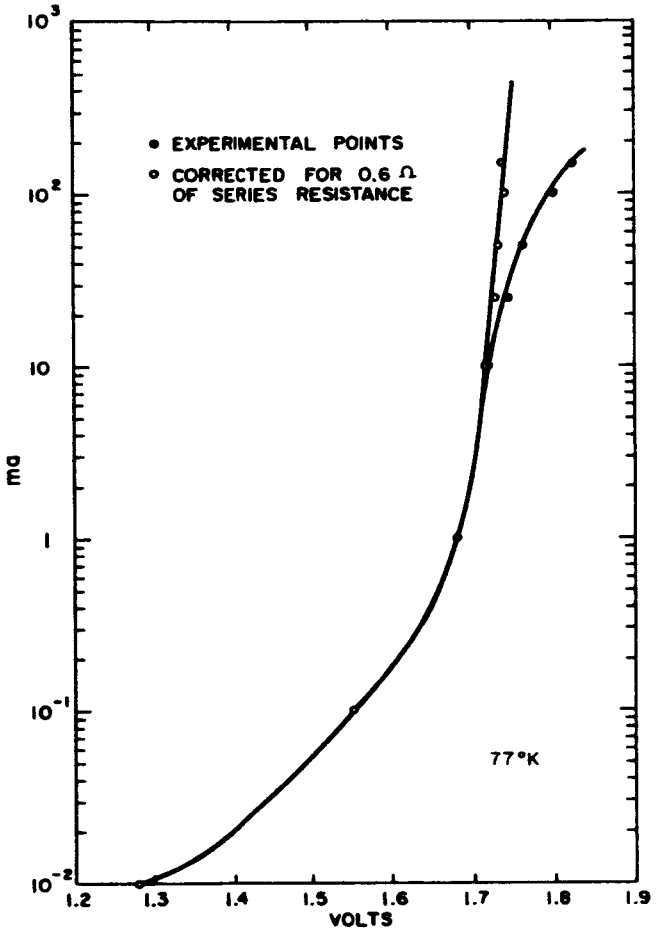

Fig. 7. Semi-logarithmic plot of current vs. voltage for $GaAs_{1-x}P_x$ diode.

the current is drawn as a function of voltage. Also shown is the curve obtained when correction is made for a 0.6-ohm series resistance. The resultant straight line has within experimental accuracy the slope predicted by simple pn junction theory for a band gap of 1.70 v at liquid nitrogen temperature (which should be a current increase by an order of magnitude for a 16-meV rise in voltage). Most diodes were found to have series resistance between 0.5 and 1.0 ohm.

Figure 8 shows (on a logarithmic plot) the variation of the light output of a typical diode as a function of current. This curve was taken by means

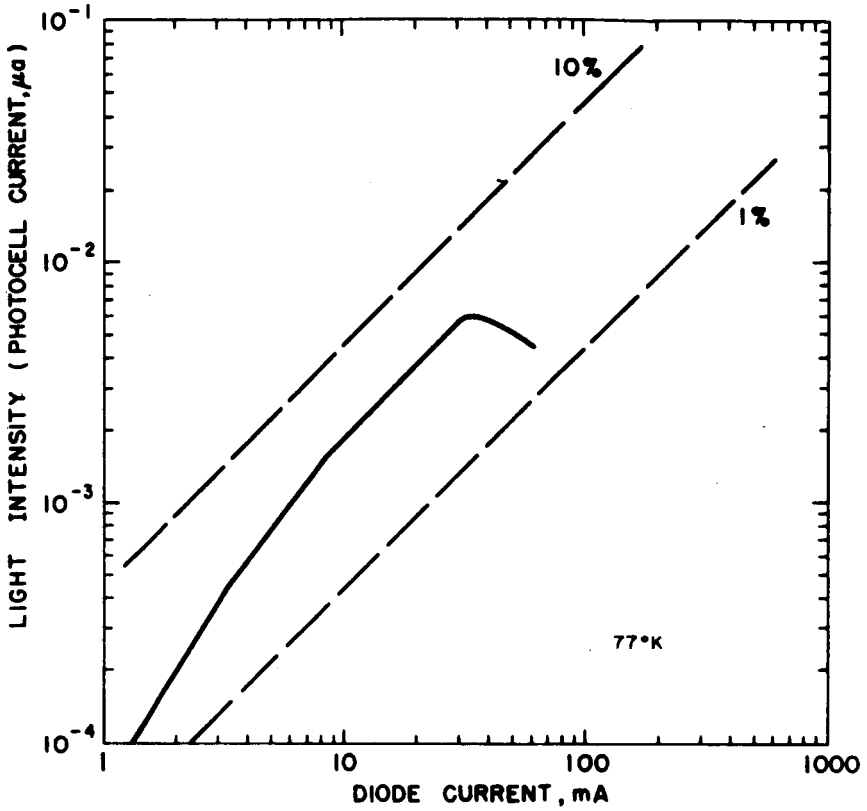

Fig. 8. Light-output vs. current for $GaAs_{1-x}P_x$ diode.

of a Tektronix Type 575 Transistor Curve Tracer which applies an oscillating voltage corresponding to a duty cycle of about one-half. The light intensity was measured with an RCA 917 photodiode which has an S-1 spectral response. Similar results are obtained at DC. It is seen that the light output at low currents increases faster than the current and then becomes proportional to the current (constant quantum efficiency). At high currents the diode heats up appreciably causing a decrease in quantum efficiency. As a result, while heating, the light intensity first rises more slowly than the current and, finally decreases with increasing current. Figure 8 also shows two straight lines corresponding approximately to 1 and 10% external quantum efficiency. The best diodes tested gave an efficiency, in terms of photons actually leaving the diode, of one to two percent. When heating is avoided, through the use of short pulses with a small duty cycle, the light remains proportional to the diode current up to much higher current levels. Figure 9 shows the light

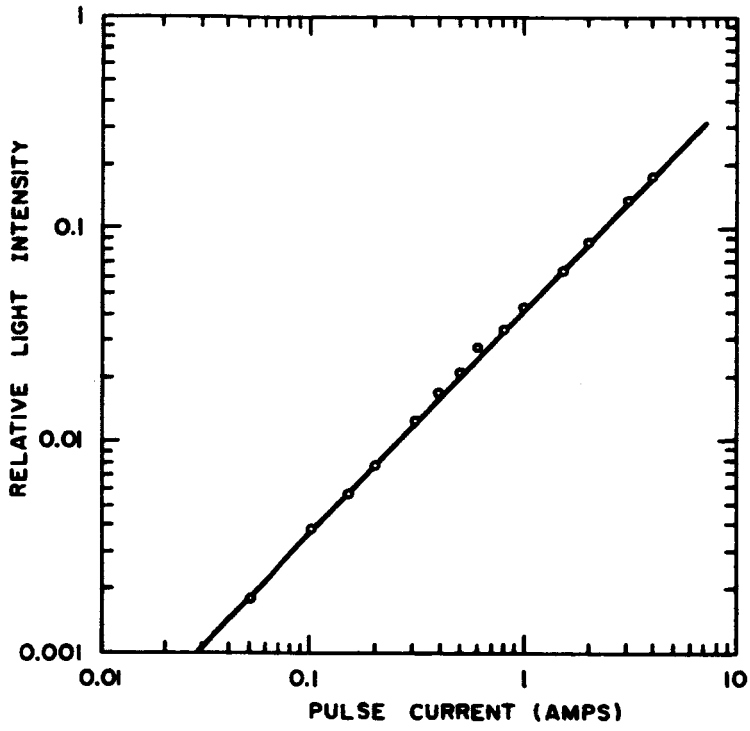

Fig. 9. Light-output vs. current for $GaAs_{1-x}P_x$ diode under pulsed operation.

output, measured in an integrating sphere, as a function of the amplitude of a square current pulse. The light intensity is approximately proportional to the current up to four amperes.

As in the case of GaAs diodes,[4] it was found that the wavelength of the emitted light at first decreases with increasing current and then becomes constant at high current values. A typical curve is shown in Figure 10a, which was taken at 27°K (liquid neon) with pulsed current. At the same time, as shown in Figure 10b, the width of the line, at half of maximum intensity, decreases. At the highest currents, where heating becomes appreciable the line width starts to increase again. Of course, a sharp decrease in line width occurs, if the lasing threshold is reached.

A typical line shape is shown in Figure 11. This curve was obtained from a different diode than that used for Figure 10. Although both diodes came from the same wafer, they differ considerably in their band gaps, indicating a variation in the GaAs:GaP ratio. Figure 11 was obtained at a current of 100 ma with the diode at 77°K.

The light output of the diodes was found to increase in intensity and decrease in wavelength with decreasing coolant temperature. This behavior is

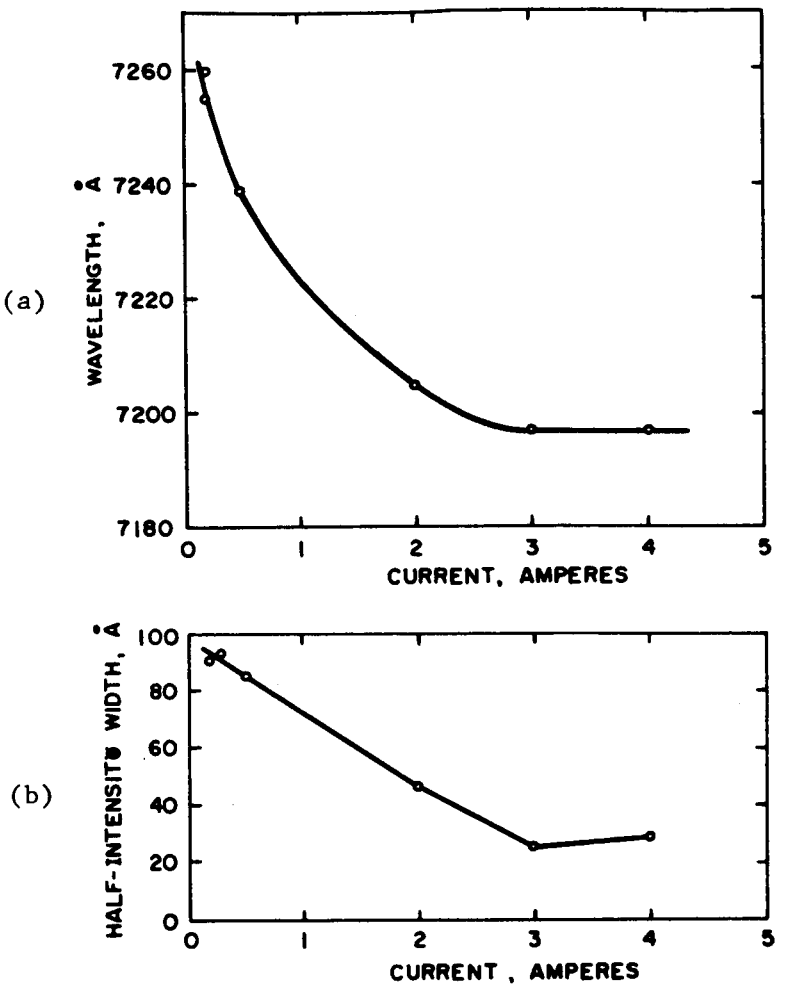

Fig. 10. (a) Photon energy and (b) Half-intensity width vs. current for $GaAs_{1-x}P_x$ diode.

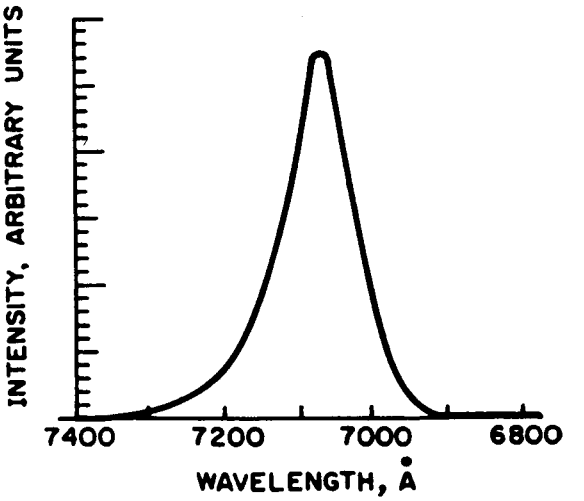

Fig. 11. Spectral line shape for electroluminescence from $GaAs_{1-x}P_x$ diode.

summarized in Table I where typical values of experimental results are indicated at four bath temperatures. It is to be noted that the actual junction temperature is somewhat higher than that of the coolant and that this temperature difference is quite appreciable when the diode is operated in air.

TABLE I

Bath Temperature (Coolant)	Knee in Forward Conduction Curve (eV)	Relative Light Intensity
4.2°K (He)	1.77	400
27 (Ne)	1.75	200
77 (N_2)	1.68	20
300 (air)	~1.4	1

Early work on these injection-luminescent diodes was aimed at large-area light sources with junction areas of the order of a square cm, which had electrodes on each side covering only part of the surface area. With these electrodes off-set, relative to each other, it was then possible to obtain reasonable light output in a direction normal to the junction plane. It was soon found, however, that this approach had several shortcomings. First, to get useful values of current density (~ 10^3 a/cm^2) a very large current source was needed and the problems of good connections, particularly at the diode electrodes were serious. Second, the diodes were found to give highly nonuniform performance over their surface area, presumably because of variations in local quantum efficiency and in the quality of the electrical contacts. Third, it was found that the efficiency obtainable, in terms of light output vs. current input, from small diodes in which the electrodes completely covered the two large faces and the light issued from the edge, was at least as high as for the large-area units. Therefore, it was decided to work with small-area units. With these it was possible to select relatively efficient diodes and to operate them in series, such that only relatively small currents (a few amperes, at most) would be drawn. It was shown that it is possible to increase the light output from these diodes by removing some of the electrode area, so that some light can issue from the large sides as well as from the edges. However, it was not feasible to perfect this technique to the point where it could be used with many diodes assembled in series-connected arrays.

Some of the diodes were found to show laser action. However, the scope of this project did not permit a concentrated effort at developing injection lasers. Lasing was observed at liquid-nitrogen temperature, but more measurements were made on a diode immersed in liquid neon. It was operated at a 60-cps rate with 1.3-μsec pulses. The threshold current density was approximately 2,000 a/cm^2. Its efficiency, in terms of actually measured light output from one face, was about 0.5%. This corresponds to an efficiency of 1% for the light issuing from both ends.

IV. LASER-PUMP ARRANGEMENT

Several preliminary arrangements were constructed for mounting $GaAs_{1-x}P_x$ diodes. The main requirements were: (1) The diodes were to be series-connected in one single string. (2) Thermal contact to the coolant bath should be good. (3) The structure had to be mechanically strong. In particular, it was necessary to keep the mechanical stresses applied to the diodes to a minimum.

In several early arrays the diodes were either soldered directly on top of each other or they were alternated with cooling vanes. The principal disadvantage of these stacks was the fact that the diodes were exposed to bending stresses and tended to break. Also, cooling was inadequate.

A more successful arrangement consisted of a comb-like structure, shown in Figure 12a, in which the diodes were mounted between a set of parallel wires.

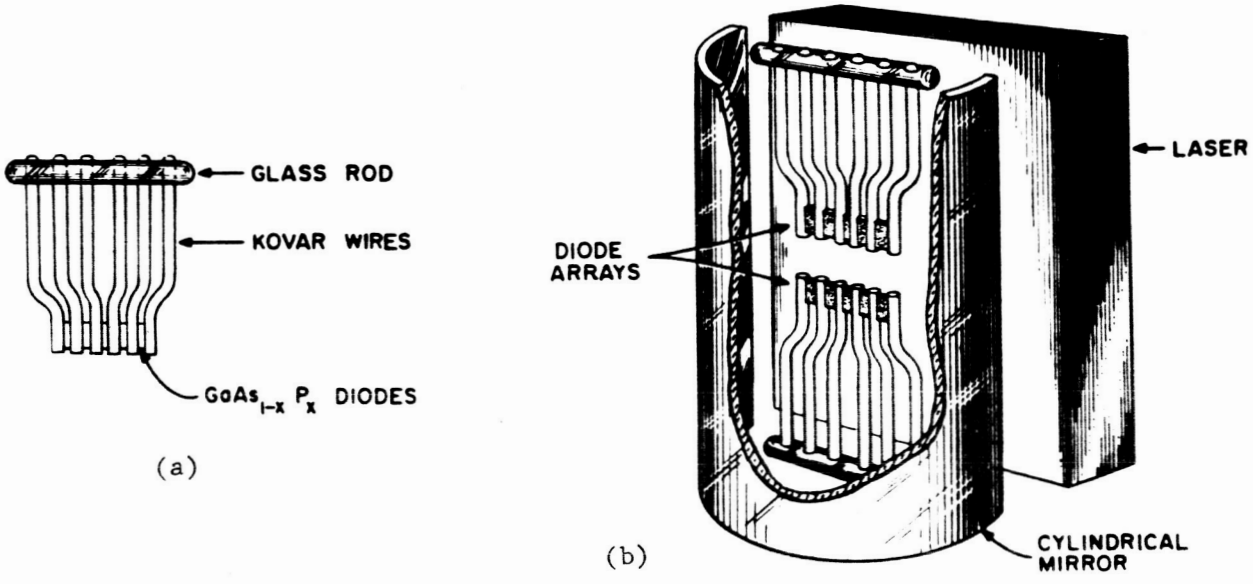

Fig. 12. (a) Diode array and (b) Mounting arrangement in early pumping scheme.

Two such units, containing a total of nine operating diodes, were mounted next to a $CaF_2:Dy^{2+}$ laser, as indicated in Figure 12b. A cylindrical mirror, placed behind the diode arrays (as shown by the dotted outline) reflected some of the light issuing from the back faces of the diodes. White incandescent light was used to pump the laser to just below its threshold. The diodes were then pulsed (with 1-millisecond pulses at a 100-cps repetition rate) which caused the $CaF_2:Dy^{2+}$ crystal to produce lasing pulses, coincident with

the driving pulses. The cross-sectional area of each diode was approximately 10^{-3} cm^2 and the current pulses had an amplitude of 3 amperes.

Later it was found that more efficient cooling could be obtained by soldering the diode between copper strips (100-mils wide and 2-5-mils thick) in a coplanar arrangement, as shown in Figure 13a. The copper strips were attached to a metallized ceramic support bar. Several such series arrays were made, each carrying ten diodes. Also, some double arrays were mounted, in which the ceramic bar carried a string of eleven diodes on each side.

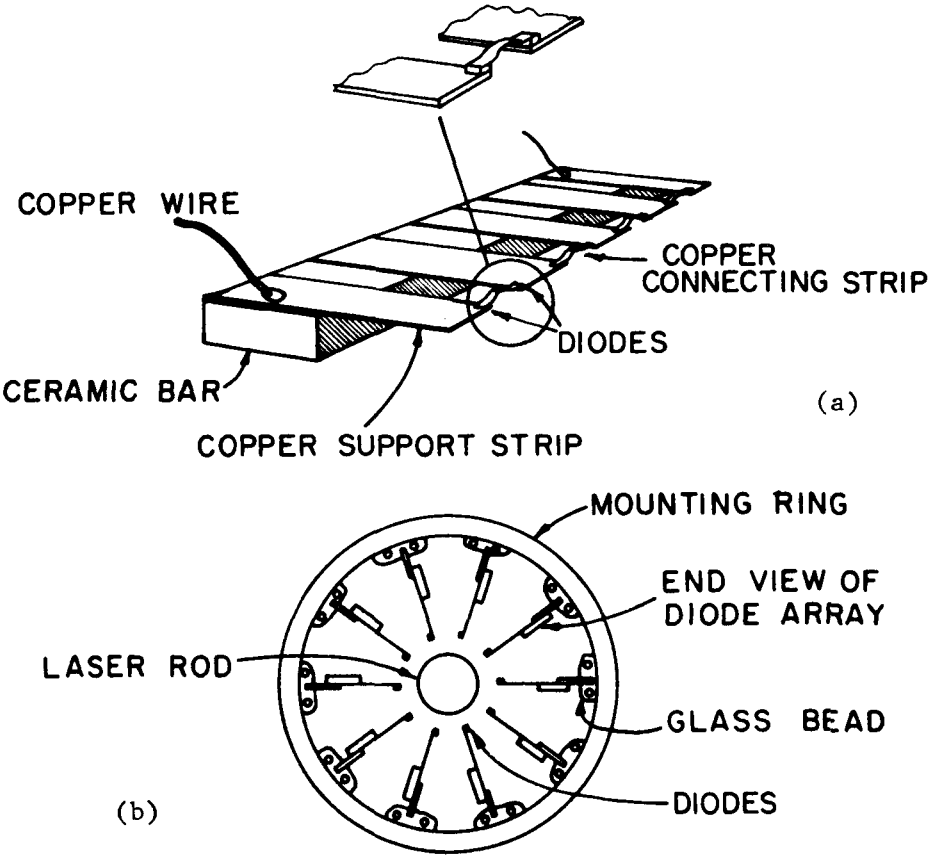

Fig. 13. (a) Linear array of $GaAs_{1-x}P_x$ diode and (b) Mounting arrangement used for pumping $CaF_2:Dy^{2+}$ laser.

Ten arrays, containing about one hundred diodes connected in series, were then mounted as shown in Fig. 13b. The laser rod was one-inch long and had a diameter of 3/16 inch. The ensemble of laser and diodes was immersed in a bath of liquid helium cooled slightly below the lambda point. Cooling the diodes to 1.9°K shortens their emission wavelength by less than 2 percent compared with the 77°K value. The output of the laser was viewed through two windows by an InAs detector located 72 cm from the laser.

Current was passed through the diodes in manually triggered single pulses whose amplitude and duration could be adjusted. A block diagram of the current supply and of the detection arrangement is given in Figure 14.

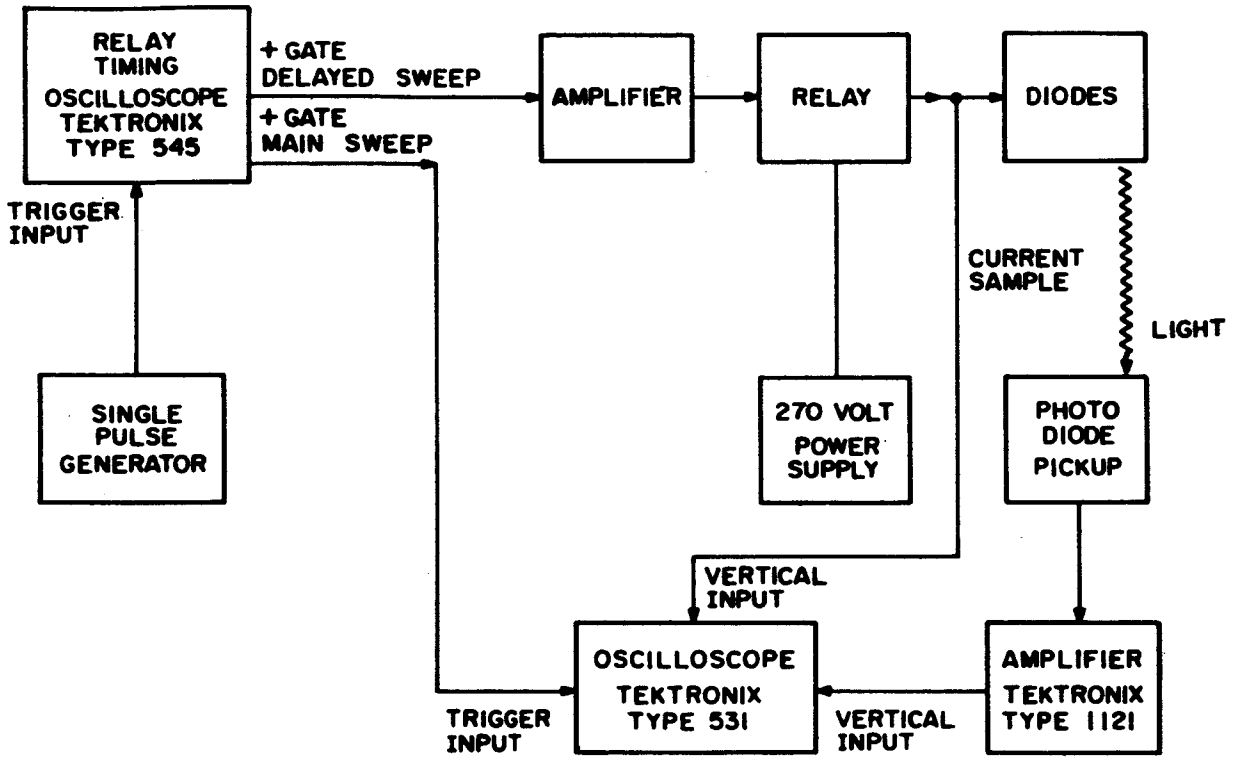

Fig. 14. Block diagram of circuit for driving laser pump and for detection of laser radiation.

Two photographs were made to show the actual structure used in this experiment. Figure 15 (a) shows two diodes within one of the linear arrays and the connecting copper strip which is bent so as to avoid stresses during temperature changes. Figure 15 (b) is a view of the complete laser-pump assembly surrounding the laser rod.

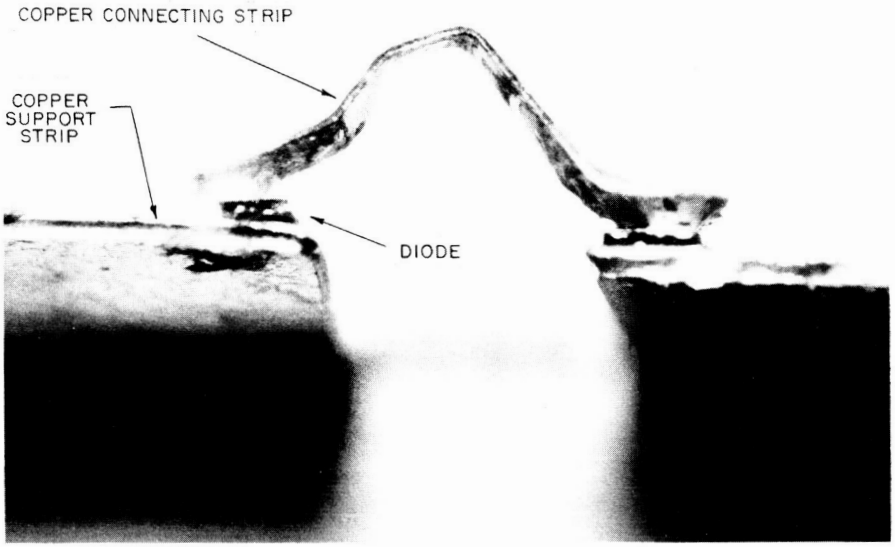

(a) Photograph of two diodes in linear array.

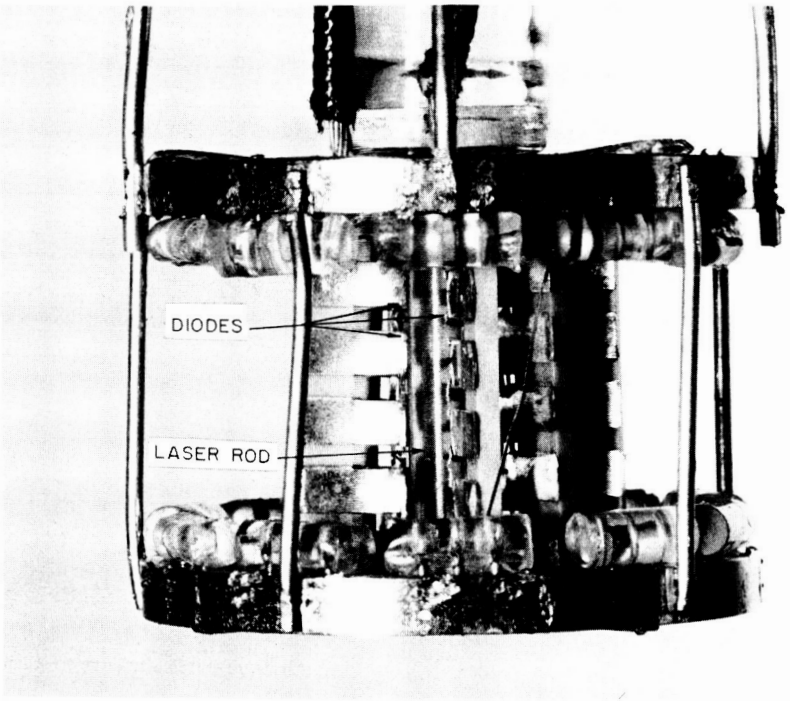

(b) Photograph of complete laser pump.

Fig. 15.

V. RESULTS

The lowest current (in 100-msec pulses) through the diodes sufficient to pump the laser was 60 ma. This corresponds to about 10 watts of electrical power supplied to the diodes or about 0.1 watt of optical pump power available for the laser (assuming a 1% conversion efficiency). Figure 16 shows a typical test result. The upper trace (a) shows the current pulse (350 ma); trace (b) shows the output of the InAs detector which indicates that in this case lasing starts 42 msec after the pumping current is turned on; and trace (c) is a display of the detector output on an expanded time scale to show the spiked output of the laser.

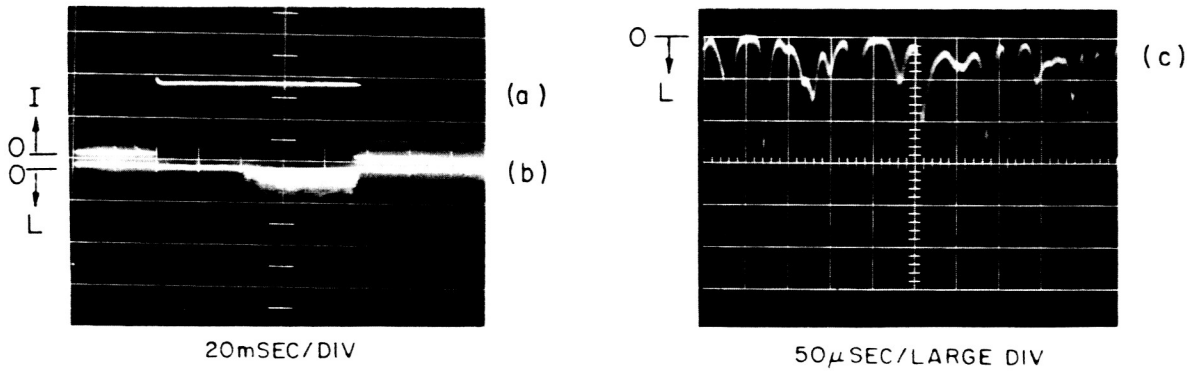

Fig. 16. Test results: (a) Current vs. time; (b) Light output (from InAs cell) vs. time; and (c) Detail of laser output showing individual spikes.

A rough measure of the power output of the laser was attempted. This was done using a PbS detector cooled to 200°K. This detector is slow enough to integrate the spiked output of the laser. In contrast to the small InAs detector, the PbS detector has a sufficiently large area to intercept the whole laser beam. The PbS detector was calibrated by comparison with a Westinghouse "Rat Nest" calorimeter using another $CaF_2:Dy^{2+}$ laser operated continuously by incandescent pumping. The power output of the injection-pumped laser, in the case shown in Figure 17 (300 ma through the diodes) is 0.16 mW.

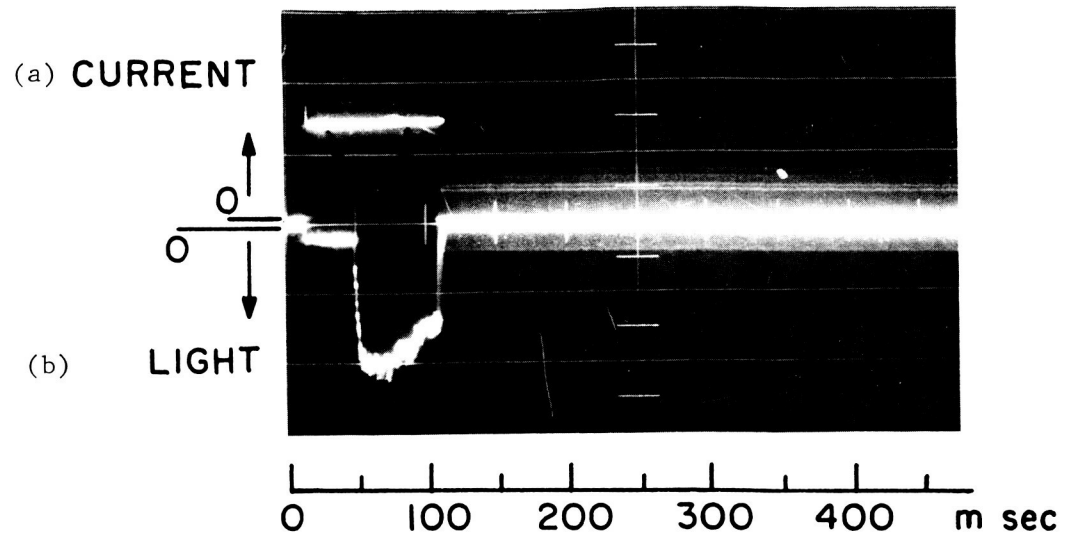

Fig. 17. Test results: (a) Current vs. time and (b) Light output (from PbS cell) vs. time, used for power measurement.

As the pumping current is increased the following effects have been observed:

1. The average pulse height of the laser spike increases.
2. The pulse density of laser output increases.
3. The delay between the beginning of pumping and the onset of lasing decreases.

The latter effect suggests a slow relaxation from the upper band to the $^5I_7$ level. The threshold is achieved when sufficient population inversion is obtained, i.e., when state $^5I_7$ contains a critical concentration N_2. If the relaxation time from the 5d level to the $^5I_7$ level is long, it can be shown that the population of the $^5I_7$ level increases linearly with the population of the 5d level, i.e., it is proportional to $\int_o^t I\,dt = It$. Hence, there is an inverse relation between the pumping current I and delay t. This is shown in Figure 18. Below 0.2 ampere the light output may not be proportional to the current.

Such long delays in lasing, i.e., such long storage time in the upper state, have not been reported before. They represent an interesting fundamental temperature-dependent property of the laser.

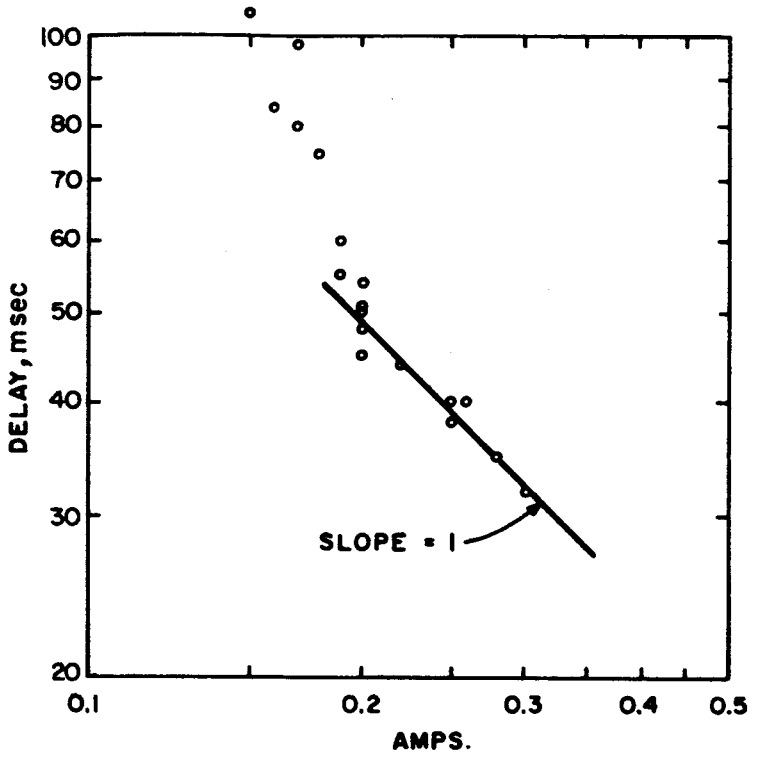

Fig. 18. Delay between start of current pulse and onset of lasing vs. pump current.

An examination of Figure 16 reveals that the coherent output of the laser continues for several milliseconds after the pumping current has been turned off. However, the delayed lasing turn-off seems independent of the pumping intensity.

VI. DISCUSSION

If the broad objective of using electroluminescence for pumping a laser has been met, there are still many unresolved problems concerning this mode of operating a laser. We shall consider some of them now.

A. MODULATION

Electroluminescent pumping offers the attractive promise of convenient modulation. The pump power is proportional to the driving current and the input impedance is low; therefore, the pump power can be varied at high frequency. However, we have seen that, at 1.9°K, the onset of lasing and its termination lag the pump power by at least a few milliseconds. Under these conditions, modulation could not be performed above a few hundred cycles per second. It is possible that at higher temperatures the laser response to pumping is much faster. This is an important property to test.

It is believed that the time lag of the laser is caused by the relaxation from the initial excitation level to the emitting level. This relaxation is probably very much faster in some other systems, particularly in $CaWO_4:Nd^{3+}$ which has an excitation band at 1.43 eV, corresponding to the photon energy of a pumping GaAs diode.

B. EFFICIENCY

The overall efficiency that we measured is of the order of 10^{-4} to 10^{-5}. This disappointing performance represents the potentials of an early state of the art. Much improvement (at least a factor of 4) should result from progress in the technology of the material and in its processing. Another one or two orders of magnitude in improvement could be achieved by going to more exotic designs (such as the Weierstrass sphere) and by using antireflecting coating. Perhaps a more practical approach would consist of using injection lasers for pumping the solid-state laser. The latter approach takes advantage of the higher output from the diode operated in the coherent mode than in the incoherent mode because of the high directionality of the output above injection threshold.

All other factors being equal, one can gain further efficiency by using a solid-state laser whose output wavelength is close to the pumping wavelength. Dysprosium is pumped at 0.72 μ and emits at 2.36 μ (at best an efficiency of

0.3). A more promising material, from this point of view, is neodymium. It is pumped at 0.9 μ and emits at 1.06 μ.

It is clear that still more work is needed before an electroluminescent pump can fulfill its promise of convenience, efficiency and modulability.

APPENDIX

EPITAXIAL GROWTH OF $GaAs_{1-x}P_x$ BY WATER VAPOR TRANSPORT

The useful and interesting electrical characteristics of GaAs and GaP are well known. A logical extension of the work on these compounds is a study of the properties of the alloys $GaAs_{1-x}P_x$. As is the case with the pure compounds (especially GaP) the alloys are difficult to prepare by normal melt-growth techniques. The usual problems encountered in the melt-growth of high-melting-point materials are concerned with purity and crystallinity. The alloys present the additional problem of homogeneity, i.e., a constant ratio of As to P throughout the matrix.

The Appendix discusses the growth of $GaAs_{1-x}P_x$:Te doped layers by a vapor-phase technique. This work was instituted in order to obtain a compound having a band gap of 1.72 eV, so that by injection luminescence it emits at 7200 Å and thereby stimulates a CaF_2:Dy laser. The difficulties inherent in the melt-growth technique, just mentioned, suggested that vapor-phase growth should be used as a preparative technique. Schaefer[5] discussed various aspects of vapor-phase transport - the preparation of high melting point materials via volatile intermediates. Antell and Effer[6] applied the technique to III-V compounds, using iodine and chlorine as the transporting agent. Pizzarello[7] synthesized large polycrystalline boules of $GaAs_xP_{1-x}$, using GaAs and P or GaAs and GaP as starting materials, and iodine as the transporting agent. Holonyak[8] reported the epitaxial growth of GaAs and GaP, using various chlorides as transporting agent. In the present work, oxygen transport was utilized, in contrast to the above worker's use of halide transport. Previous experience[9] with the transport of GaAs via Ga_2O, in a close-spaced system, indicated that Ga compounds can be successfully transported in this manner. Therefore, the close-spaced system with water vapor as the source of oxygen seemed the logical choice of method.

EXPERIMENTAL

The close-spaced system of F. H. Nicoll[10] was used, as shown in Figure 19. The source and substrate wafer temperatures were each controlled by separate heaters. To ensure an equal temperature over the entire wafer, heavy molybdenum

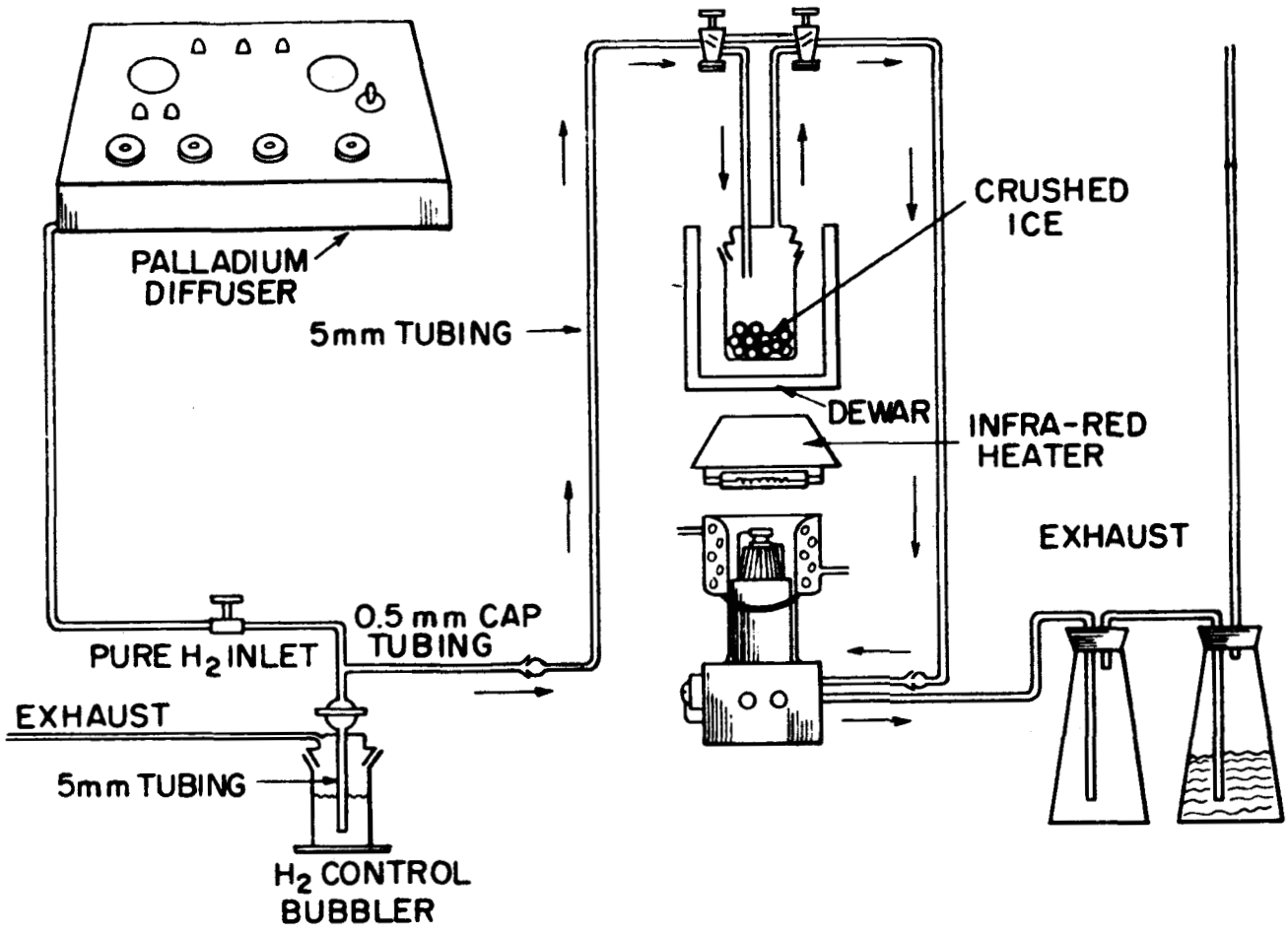

Fig. 19. Close-spaced system and associated control apparatus.

discs were placed between the wafers and their respective heaters. Temperature measurements and control were achieved by thermocouples placed in small holes in the molybdenum discs. The temperatures ultimately utilized were 935°C in the hot zone (source) and 920°C in the cold zone (substrate). A spacing of 10 mils was used between the source and substrate. Palladium-diffused hydrogen, at a flow rate of 6 cc/minute, was passed over ice at -20° to -30°C; the temperature was maintained by a salt-ice bath, or by an ethylene glycol-water bath. This technique controlled the amount of water vapor admitted to the system. The various growth parameters were studied by observing the weight loss of the source wafer, as a function of the parameter of interest. A detailed description of the apparatus and of the experimental procedure has been given previously.[9]

The $GaAs_{1-x}P_x$:Te source wafers were cut from melt-grown ingots. These source wafers were polycrystalline, with a varying As-P ratio. Powdered

$GaAs_{1-x}P_x$ mixtures were also used as sources; however, the work reported here utilized only melt-grown sources. Mechanically polished (111) and (100) GaAs wafers, etched in 1:1:10 $H_2O:H_2O_2:H_2SO_4$ prior to growth were used as substrates.

RESULTS AND DISCUSSION

The reaction which makes the formation of the crystalline layers possible is a transport of $GaAs_{1-x}P_x$, assumed to proceed as follows:

$$2\ GaAs_{1-x}P_x + H_2O \rightleftarrows Ga_2O + (1-x)\ As_2 + (x)\ P_2 + H_2 \qquad (1)$$

Ga_2O is the actual transporting species, as demonstrated by several authors.[11, 12] It was previously found that the transport of GaAs by H_2O is proportional to $\sqrt{P_{H_2O}}$; this study shows that $\sqrt{P_{H_2O}}$ vs. amount of $GaAs_{1-x}O_2$ transported (Figure 20) is also a straight line.

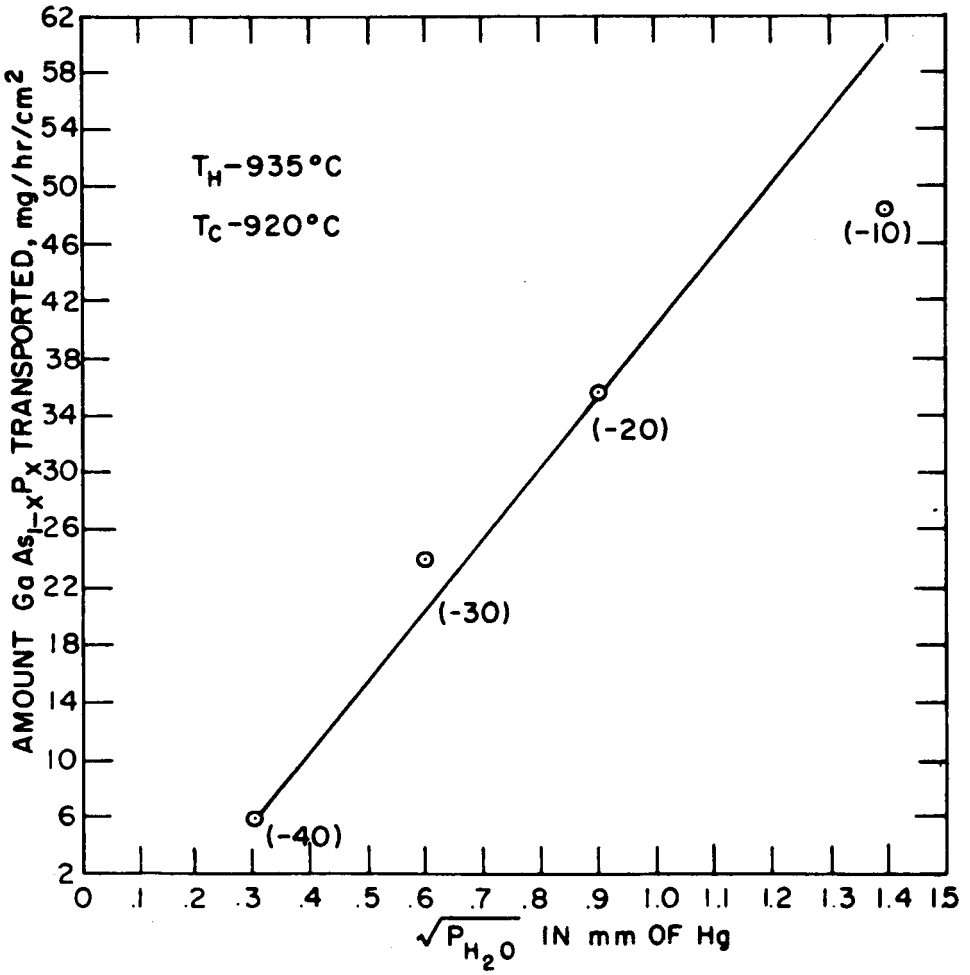

Fig. 20. Amount transported vs. square root of water-vapor pressure.

The layers of $GaAs_{1-x}P_x$ obtained in this study were single-phase, single-crystal solid solutions of the above-mentioned material. Optimum growth rate is necessary to produce the best layers. If the growth rate is maintained at one mil/hour, a completely mirror-like layer is obtained. Between one and four mils/hour the appearance of the layer changes from a matte finish to a very rough finish. At a growth rate greater than 4 mils/hour, polycrystallinity is encountered.

Among the factors influencing growth rate are source composition, temperature of source and substrate, temperature difference, and wafer geometry. A good growth rate in itself is not sufficient to produce useful layers. Other factors of importance are substrate perfection, doping and impurities in the films.

It was observed that as the temperature difference between source and substrate is decreased, the amount transported also decreases. This is shown in Figure 21. The dependence of the amount of $GaAs_{1-x}P_x$ transported on the

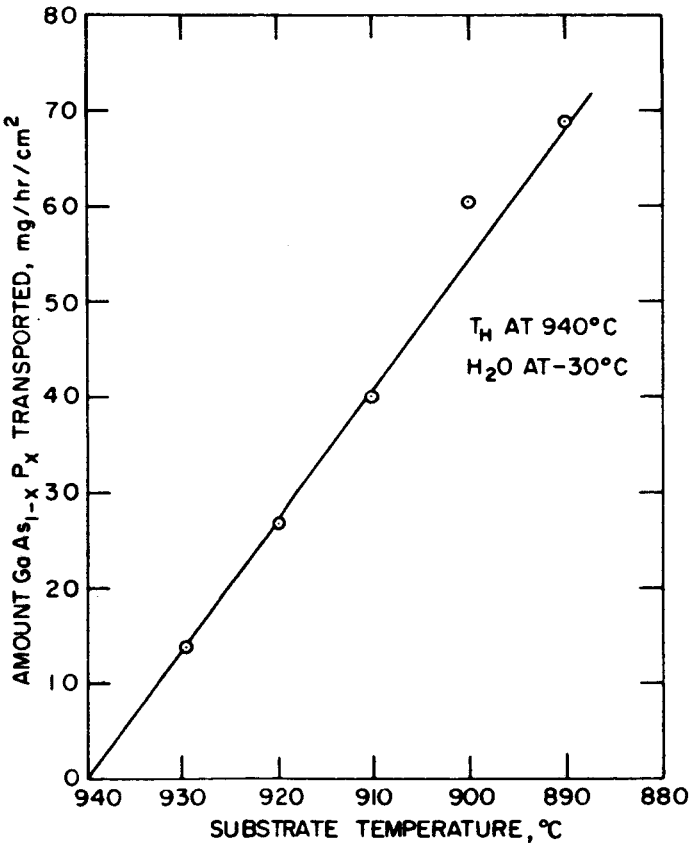

Fig. 21. Amount transported vs. substrate temperature at constant source temperature.

substrate temperature (temperature difference) is due to the close spacing, and the resultant interaction between source and substrate parameters. In a large flow system in which the source and substrate are in separate "compartments" the amount transported is a function of the source temperature under a given set of conditions. This is because the concentration of Ga_2O in the gas phase is dependent only on the source temperature. The substrate temperature will determine the amount of material deposited. Any Ga_2O which does not form $GaAs_{1-x}P_x$ in the lower temperature area is subsequently swept out of the system by the carrier gas and will obviously have no further effect on the processes occurring. The above situation can exist because true chemical equilibrium is not attained, and therefore, the forward and reverse reactions proceed almost independently of each other. This is not true in a sealed system. Equilibrium is reached quickly, and any Ga_2O that does not form $GaAs_{1-x}P_x$ in the low temperature area increases the concentration of Ga_2O in the gas phase so that ultimately the formation of Ga_2O, i.e., the forward reaction in equation (1) slows down. This is manifested as a smaller weight loss of the source and consequently a smaller amount of $GaAs_{1-x}P_x$ transported. The close-spaced system approaches the behavior of a sealed system, in this respect, and therefore, the substrate temperature, by affecting the concentration of Ga_2O in the gas phase, has a profound effect on the amount of $GaAs_{1-x}P_x$ transported, as shown in Figure 21.

Most of the source wafers were Te doped in the 1-5 x 10^{18} atoms/cm^3 range; however, 10^{17} Te/cm^3 doping was also studied. Both mass spectroscopy and electrical measurements indicated that in the range 10-100 parts per million (2 x 10^{17} - 2 x 10^{18}), the Te concentration in the epitaxial layer is the same as that in the source wafer. However, source wafers with up to 300 ppm of Te produced epitaxial layers containing only 100 ppm. These data are shown in Table II. Since the vapor pressure of elemental Te is large, it is not clear whether the Te transports as Te or as TeO_2.

The uniformity of the grown layers was studied by ultrasonically cutting small discs (0.040-in. diameter) from two wafers and then analyzing the composition of these discs via lattice constant measurements. In one wafer (Figure 22b), it was found that the maximum variation in composition was 2% (73.4 to 75.4% GaAs.) Most of the wafer was 75.4%, with the 73.4% region being very small. The diffraction lines are sharp, indicating a variation

TABLE II

Wafer Number	Oxygen content of source ppm	Oxygen content of grown layer ppm	Tellurium content of source ppm	Tellurium content of growth layer ppm	Substrate temp. °C	Growth rate $mg/hr/cm^2$
32	—	330	100	100	900	100
84	3	135	10	10	920	38.4
97	3	1350	10	10	945	16.9
116	—	1300	100	100	920	23.3
122	—	—	7.5×10^{17}*	2×10^{18}*	920	24.8
124	—	135	—	10	920	29.7
126	10	400	—	29	945	—
143	30	—	300	100	920	20.4
150	30	330	300	100	920	20.4

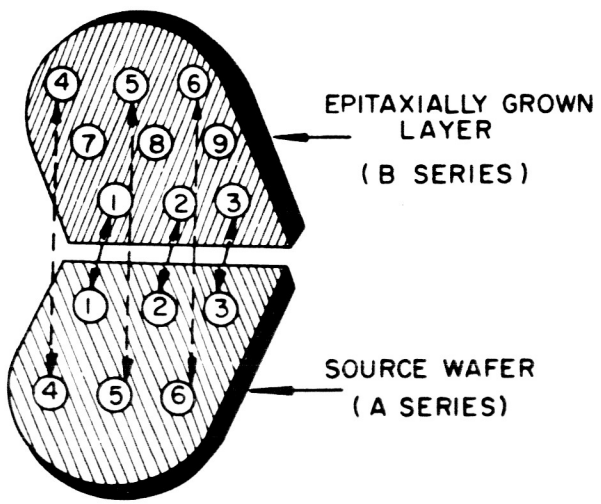

Sample	Lattice Constant Å	Mole % GaAs	Mole % GaP
B_1	5.592	69.9	30.1
B_2	5.596	71.7	28.3
B_4	5.596	71.7	28.3
B_5	5.591	69.3	30.7
B_6	5.596	71.8	28.2
B_7	5.593	70.5	29.5
B_8	5.595	71.0	29.0
A_1	5.586 - 5.607	67.0 - 77.2	33.0 - 22.8
A_2	5.580 - 5.598	64.0 - 72.6	36.0 - 27.3
A_5	5.584 - 5.609	66.0 - 78.0	34.0 - 22.0
A_6	5.581 - 5.603	64.4 - 75.2	35.6 - 24.8

Fig. 22. Compositional variation in grown layer compared to variation in source.

within each disc, of less than $\pm$ .5%. The second wafer was also studied via lattice constant measurements on ultrasonically cut discs. The source wafer from which it was produced was also cut up and studied. The results of both analyses are shown in Figure 23. It is observed that both the internal variation, and overall variation are much less in the grown layer than in the source.

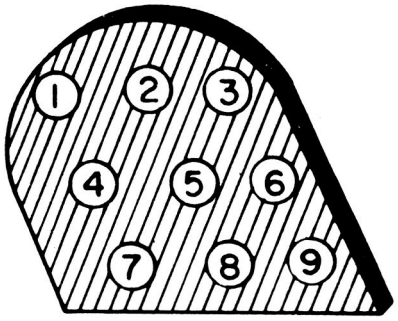

Sample	Lattice Constant Å	Mole % GaAs	Mole % GaP
1	5.6033	75.4	24.6
3	5.6033	75.4	24.6
4	5.5991	73.4	26.6
5	5.5991	73.4	26.6
6	5.5991	73.4	26.6
7	5.5991	73.4	26.6
8	5.5991	73.4	26.6
9	5.5991	73.4	26.6

Fig. 23. Compositional variation in grown layer.

In a transport reaction the amount of transporting agent incorporated into the grown layer is of interest. For this purpose, mass spectrographic studies were utilized. Table II shows that the source wafers were reasonably low in oxygen concentration. The oxygen content of the grown layers was found to be 100-1000 ppm, or 0.01-0.1 atomic percent. This is the same range that previous workers[15] found for the incorporation of halide transporting agents in halide vapor grown III-V compounds. A recent report[16] indicates that molybdenum is attacked by oxygen at 550°C; mass spectrographic analysis did not show the presence of any molybdenum in the epitaxial layers. This indicates that the reaction of water vapor with $GaAs_{1-x}P_x$ is favored over the molybdenum reaction.

As was mentioned previously, single-crystal, single-phase layers of $GaAs_{1-x}P_x$:Te were grown using powdered sources. Both powdered $GaAs_{1-x}P_x$, and GaAs plus GaP were used. Preliminary investigations on the uniformity of these layers indicate that they are at least as homogeneous as the layers grown from melt-grown source wafers.

REFERENCES

1. Z. J. Kiss and R. C. Duncan, Jr., Proc. IRE 50, 1531 (1962).
2. J. I. Pankove and M. Massoulie, J. Electrochem. Soc. 11, 71 (1962).
3. N. Holonyak, Jr. and S. F. Bevacqua, Appl. Phys. Letters 1, 82-83, (1962).
4. J. I. Pankove, Phys. Rev. Letters 9, 283 (1962).

   G. C. Dousmanis, C. W. Mueller, and H. Nelson, Appl. Phys. Letters 3, 133 (1963).
5. H. Schafer, H. Jacob, and K. Etzel, Z. Anorg. and Allg. Chem. 286, 27 (1956) ibid, 42.

   H. Schafer and B. Morcher, Z. Anorg. and Allg. Chem. 290, 279 (1957).
6. G. R. Antell and D. Effer, J. Electrochem. Soc. 106, 509 (1959).
7. F. A. Pizzarello, J. Electrochem. Soc. 109, 226 (1962).
8. N. Holonyak, Metallurgy of Semiconductor Materials (Interscience Publishers, New York 1962) p. 49
9. G. E. Gottlieb and J. F. Corboy, RCA Review 24, 585 (1963).
10. F. H. Nicoll, J. Electrochem. Soc. 110, 1165 (1963).
11. S. Antkiv and V. H. Dibeler, J. Chem. Phys. 31, 1890 (1953).
12. C. J. Frosch and C. D. Thurmond, J. Phys. Chem. 66, 877 (1962).
13. W. J. McAleer, H. R. Barkemyer, and P. I. Pollak, J. Electrochem. Soc. 180, 1168 (1961).

    G. R. Antell, J. Appl. Phys. 31, 1686 (1960).
14. E. A. Golbransen, K. F. Andres, and F. A. Brossart, J. Electrochem. Soc. 110, 952 (1963).